УДК 544.4-022.532; 544.726; 620.3

Effect of particle size and content of the metal on the oxygen reduction by silver–ion exchanger nanocomposites

Khorolskaya S.V., Kravchenko T.A., Peshkov S.V.

Voronezh State University, Voronezh, Russia

Received 5.12.2013 г.

Аннотация

This paper reports obtaining the new silver-containing nanocomposites based on the ion exchangers with the controlled size of metal nanoparticles and metal content. The redox sorption of oxygen dissolved in water by silver-containing nanocomposites with metal particles of different sizes and metal content is considered. The kinetic study showed that the rate of molecular oxygen reduction increases with the decrease of silver nanoparticles size and silver content in the NC.

Keywords: Nanocomposite, metal nanoparticle, ion exchanger, oxygen reduction reaction, redox sorption, kinetics, size effect, precursor, silver.

В работе сообщается о получении новых серебросодержащих нанокомпозитов на основе ионообменников с контролируемым размером наночастиц металла и содержанием металла. Рассматривается процесс восстановительной сорбции растворенного в воде кислорода серебросодержащими нанокомпозитами с частицами металла разного размера и содержания. Кинетические исследования показали, что скорость восстановления молекулярного кислорода возрастает с уменьшением размера частиц серебра и содержания серебра в нанокомпозите.

Ключевые слова: нанокомпозит, наночастица металла, ионообменник, реакция восстановления кислорода, редокс-сорбция, кинетика, размерный эффект, прекурсор, серебро

Introduction

Nowadays the functional nanosize materials of the new generation are produced increasingly in order to find the ways of progress in the chemical technology. Nanocomposite (NC) polymers are especially promising among materials in which metal nanoparticles (or their compounds) are introduced into the porous matrix (support) with fixed ion-exchange centers [1-11]. The extended surface of the metal nanoparticles and high reactivity increase the efficiency of a wide variety of catalytic, electrocatalytic, sorption and biochemical processes [12-16]. For example, ion exchangers with metal oxide nanoparticles with the unique sorption and magnetic properties for sensing heavy metal ions and sorption of environmental contaminants were obtained by SenGupta and co-workers [12, 13]. Also it is demonstrated by Muraviev et al. [8, 9] that bimetallic catalytically active NCs can be used as an active element of sensors for H_2O_2 detection. NCs, which combine ion-exchange and redox properties, are able to deoxygenate water [17-20]. The target attribute of such materials is their bifunctionality [12-14]: the ionogenic

centres of the polymer represent the inner source of the ionic reagents and the sink for the ionic products. The multifunctional composite systems can be arranged into a self-assembling structure by means of the templated substrates [21].

As previously established [17], the reaction rate is determined by both the nature of the metal and its level of dispersion. It was calculated in the case of copper-containing NCs, that the dimensional factor plays an important role until the process moves completely into the area of the internal diffusion kinetics; i.e., until it reaches the maximum possible rate.

Therewith it is noted [22] that, starting from the certain critical metal content, its state ceases to be a set of isolated particles. The metal forms an assembly of clusters, in which the transfer of the charge is possible with the optimal distance between the particles. This factor must be taken into account, because it leads to the dramatic change in the rates of stages, including the charge transfer and ion transport. Consequently, it is very important to find the relation between the size of the embedded metal particles, the metal content in the ion-exchanging matrix and the kinetic mechanism of the chemical reaction with their participation.

The purpose of this paper is to study the kinetics of the redox sorption (ROS) of the molecular oxygen dissolved in water by the silver–ion exchanger nanocomposites depending on the size of incorporated metal nanoparticles and the metal capacity.

Experimental

For the synthesis of nanocomposites the sulfonic type cation exchanger KU-23 15/100 (copolymer of styrene with 15% divinylbenzene, Azot Ltd., Cherkassy, Ukraine) with an ion-exchange capacity ε_{H^+} of 1.25 mmol/cm^3 was used. The grain size was R_0 = 0.45 ± 0.02 mm (pore size: 5–100 nm).

The synthesis of metal nanoparticles in the polymer macroporous matrix of the sulfonic type cation resin (KU-23) occurs in three stages: (1) saturation of the resin by metal cations (by using 0.05 M $AgNO_3$); (2) metal precipitation in the polymer (precursor formation by using 1.6 M KCl, 1.6 M KBr, 1.6 M KI, 0.63 M NaOH); (3) reduction to the zero valent state (by using 0.34 M N_2H_4, 0.08 M $NaBH_4$, H_2):

$$zR^-H^+ + Me^{z+} \rightarrow R_z^-Me^{z+} + zH^+ \quad (1)$$

$$R_z^-Me^{z+} + zNaX \rightarrow [R^-Na^+]_z\, MeX_z \quad (2)$$

$$[R^-Na^+]_z\, MeX_z + Red \rightarrow [R^-Na^+]_z\, Me^0 + Ox + zX^-, \quad (3)$$

where R^- is the polymer matrix with negatively charged sulfonate groups, $X^- = Cl^-, Br^-, I^-, OH^-$, Red is the reducing agent. After receiving metal particles in the ion exchanger, the patterns were transformed into the H^+-form by means of the contact with 0.06 M H_2SO_4. Between each of these steps the ion exchanger was washed out by distilled water. The water and the acid solution were deaerated by the argon to prevent an oxidation of NC. The amount of silver deposited inside the matrix was estimated by the complexometric method with ammonium thiocyanate (with Fe^{3+} ions as an indicator). Solutions for the titration analysis were obtained by the dissolution of a known amount of NC in several portions of boiling 10 wt% HNO_3.

The distribution of metal particles, including the average size, was obtained by Scanning Electron Microscopy (SEM, Jeol JSM-6380) and X-ray analysis with DRON-3 diffractometer. Sliced NC grains were attached with the conducting graphite glue to the lead substrate for SEM studies and for Energy Dispersive Spectrometry (EDS). EDS was carried out by using Jeol JSM-6380 to analyse the metal distribution along the radial

direction of the granule. For this, 5-6 areas of 3,4 μm^2 were selected passing from the grain centre to its periphery, with the accumulation time of 50 s in each area.

X-ray diffractograms of nanocomposites (dispersed up to powder state) and of the massive metal were registered for 2Θ angles from 10° till 70° with scan rate of 2° per min (accumulation time: 3 s) with Cu Kα source, λ = 0.154 nm. For precise determination of the peak broadening, diffractograms were re-measured in the vicinity of the (111) peak with scan rate of 0.25° per min. The coherent scattering length for nanocrystals in the composite being found from broadening of its (111) peak compared to that of the massive metal. The value of the peak broadening was inserted into the Scherrer equation.

The degree of the oxygen sorption $\alpha = Q(t)/Q_{max}$ was measured by the gasometric method described elsewhere [17]. The measurement in this method is based on the determination of the oxygen volume change in the reaction chamber with the stirred distilled water and NC grains. The constant concentration of oxygen dissolved in water was maintained. The reacting system was in equilibrium at a constant temperature (T = 293 K), and oxygen pressure was equal to atmospheric pressure. The quantity of the granulated NC in the experiment was 1 cm^3.

Results and discusion

The chemical deposition of metals in the ion exchangers allows us to obtain composite materials containing nanostructured metals in their structure. Metal particles stabilized within a sulfonic type cation exchanger are complex formations that are actually aggregates of smaller nanostructured particles. The investigation of the samples shows from the X-ray analytical data, that nanometer particles in the size range 10-100 nm are distributed inside the NC (Table 1), with a portion of the nanoparticles joined into aggregates. Therefore, the particle sizes found microscopically are overestimated; due to difficulties in discrimination the interfacial boundaries in the above mentioned polycrystallites.

By applying particular conditions for the chemical deposition of metal in a macroporous sulfocation exchanger, it is possible to obtain Ag^0·KU-23, in which the size of the metal component is controlled. The influence of two factors, precursor and reducing agent, on the size of metal nanoparticles is shown further. The formation of the first solid-phase product, or precursor, which predetermines the structure of the particles of the deposited metal [24], plays the most important role in the process of preparing a NC.

Table 1. Average diameter of Ag particles d in Ag^0·KU-23(H^+) nanocomposites depending on the nature of the precursor and the reducing agent, as determined by Scanning Electron Microscopy (SEM) and X-ray diffraction

NC	Reducing agent	Precursor	ε_{Ag^+}, mmol cm^{-3}	Solubility product at 25 °C [23]	d, nm	
					SEM	X-ray
Ag^0·KU-23	N_2H_4	AgCl	0.80 ± 0.03	$1.6\cdot10^{-10}$	260	97
		AgBr	0.76 ± 0.02	$7.7\cdot10^{-13}$	130	72
		AgI	0.81 ± 0.03	$1.5\cdot10^{-16}$	96	37
	$NaBH_4$	AgOH	0.82 ± 0.03	$1.9\cdot10^{-8}$	96	30
	H_2	Ag^+	0.31 ± 0.02	-	66	10

In order to estimate the influence of the type of precursor on the mean size of silver particles, the samples obtained from silver halides, namely, chloride, bromide, and iodide,

were investigated. In addition, all the above samples were also characterized by the function of the particle size distribution according to their sizes in the grain volume of NC on the basis of microphotographs obtained by SEM. It was found from these microscopic observations that in all these cases, spherical particles (aggregates) of silver of various sizes (Table 1) are formed with a normal size distribution. Not only the mean size of silver particles is reduced, but also their size distribution narrows according to the following series of precursor compounds AgCl > AgBr > AgI (Figure 1a).

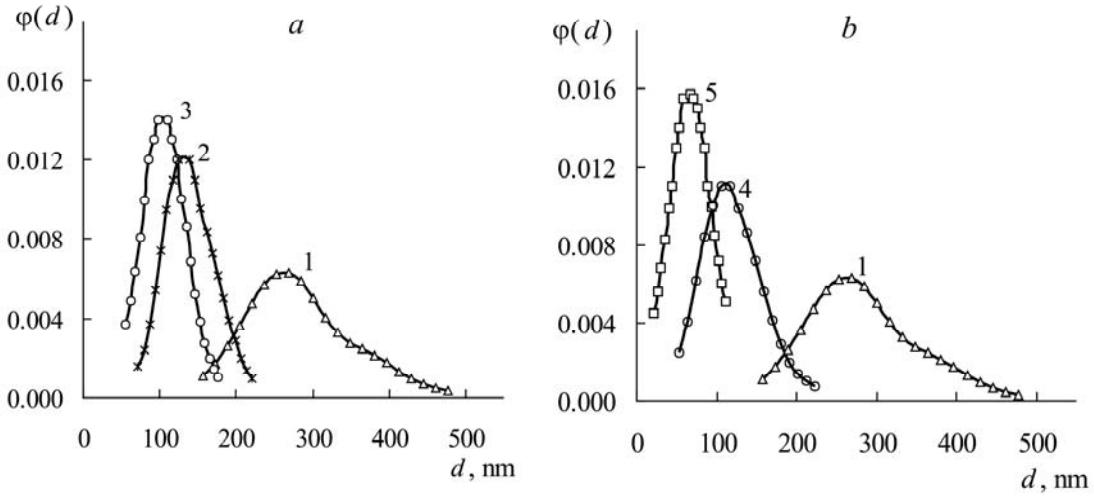

Fig. 1. Function of the distribution of silver particles by size d for Ag^0/KU-23 NCs synthesized using different precursors (*a*) and reducing agents (*b*): 1 – AgCl precursor, N_2H_4 reducing agent; 2 – AgBr precursor, N_2H_4 reducing agent; 3 – AgI precursor, N_2H_4 reducing agent; 4 – AgOH precursor, $NaBH_4$ reducing agent, 5 – Ag^+ precursor, H_2 reducing agent.

In a series of the precursors AgCl > AgBr > AgI [25], the solubility product of the precursor compounds (Table 1) decreases, and their aggregate stability increases. Consequently, the supersaturation of the solution in pores reduces that leads to the decreasing of silver ions concentration, which participate in the following nucleation.

The second factor that controls the size of metal particles in NCs is the nature of the reducing agent. In samples obtained using hydrazine, ($E^0_{N_2/N_2H_4}$ = –0.31 V [26]), the mean size of silver particles is 100–200 nm, and when sodium borohydride is used ($E^0_{NaB(OH)_4/NaBH_4}$ = –0.40 V [26]), the sizes are in the range 80–100 nm. The composite that was reduced by gaseous hydrogen has the smallest size of silver particles, which is equal to 40–70 nm (Figure 1b). It also has the lowest metal content and the most uniform grain distribution (Figure 2).

The redox potential of a solution of the reducing agent and the pH value during precipitation play a crucial role from the point of view of thermodynamics. The shift of the redox potential of the reducing agent towards more negative values fosters the increase in the dispersity degree of the produced metal particles. It means that the potential difference of the two partial reactions of the oxidation of the reducing agent and the reduction of the metal ion increases. Increasing the pH of solution shifts the potential of the concerned half-reaction to more negative values. Therefore, strongly alkaline solutions of the reducing agents with high pH values were chosen for the synthesis.

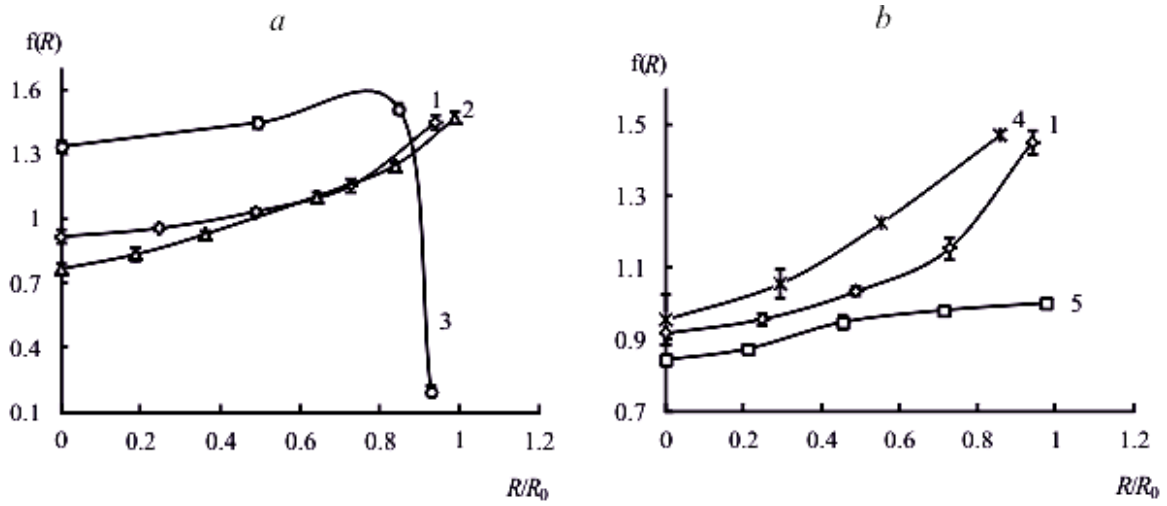

Fig. 2. Dependence of the relative content $f(R)$ of silver on the radial coordinate R of a NC grain with radius R_0, (designations for the curves are the same as Fig. 1).

According to X-ray spectral microanalysis, the content of silver is distributed nonuniformly along different points of the grain radius and increases from the center to its surface in all the silver-containing materials, with the exception of the sample synthesized with hydrogen. This is shown by the dependency of relative concentration of silver on the radius of the NC grain (Figure 2).

A study of the reduction of oxygen with silver-containing NCs showed a substantial increase in the process rate with the increasing dispersity of silver particles. Figure 3*a* shows the kinetic curves for the completeness degree α of the oxygen ROS by Ag^0·KU-23 with different microscopically determined mean sizes of silver particles. The increase in the process rate is not entirely obvious in the case of samples, which are synthesized using silver bromide and iodide precursors. The reason of this phenomenon is the presence of specifically adsorbed components that remain after the reduction of the NC at the stage of its synthesis. Thus, peaks corresponding to AgI are observed in the X-ray patterns (Figure 4).

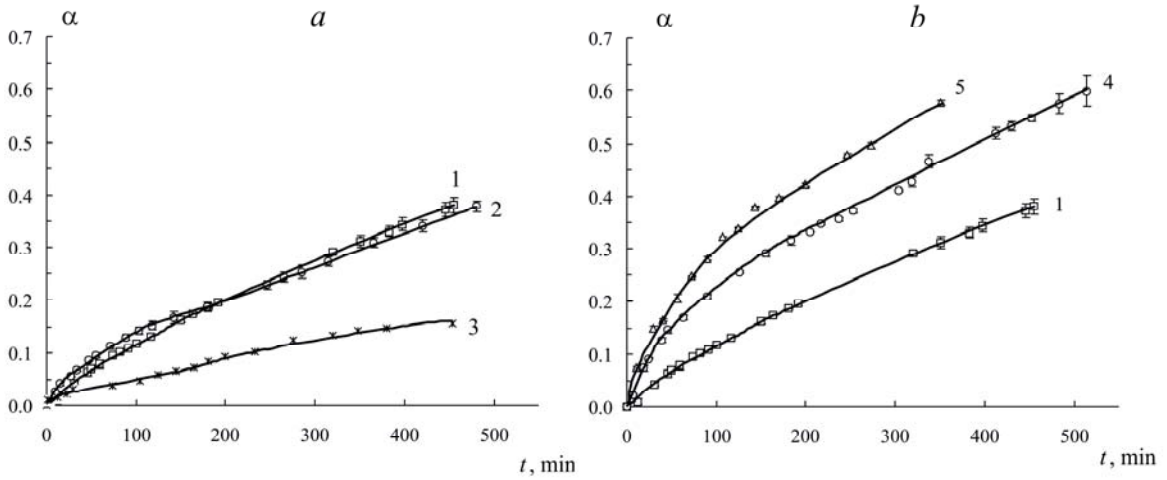

Fig. 3. Kinetic curves for the process completeness degree 'α' of the ROS of molecular oxygen from water by Ag^0·KU-23 in H^+-ion form, obtained by chemical deposition of silver with different precursors (*a*) and reducing agents (*b*) (curves designations as Fig.1).

At the same time, the expected relationships are markedly observed in the experimental curves for the samples reduced by hydrazine (with AgCl precursor), sodium borohydride, and hydrogen (Figure 3b). The sample synthesized using hydrogen is the most reactive. As it was noted above, it is characterized by the smallest size of silver particles in the studied series of materials.

In general, the completeness degree of the oxygen ROS for a certain process time (100 min) demonstrates that the reactivity of the silver particles increases with an increase in their dispersity degree (Fig. 5).

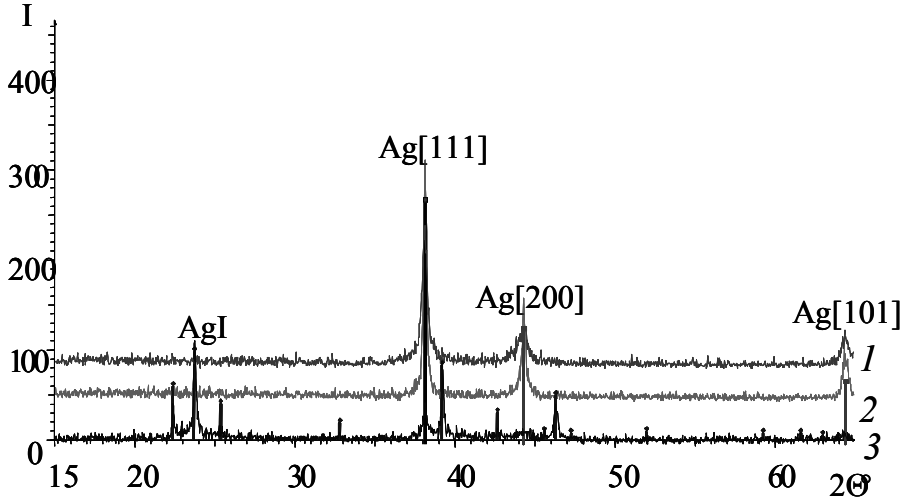

Fig. 4. Peaks of different crystallographic planes in the X-ray diffraction patterns of Ag^0·KU-23 with different precursors: AgCl (1), AgI (3); and reducing agents: N_2H_4 (1, 3), $NaBH_4$ (2)

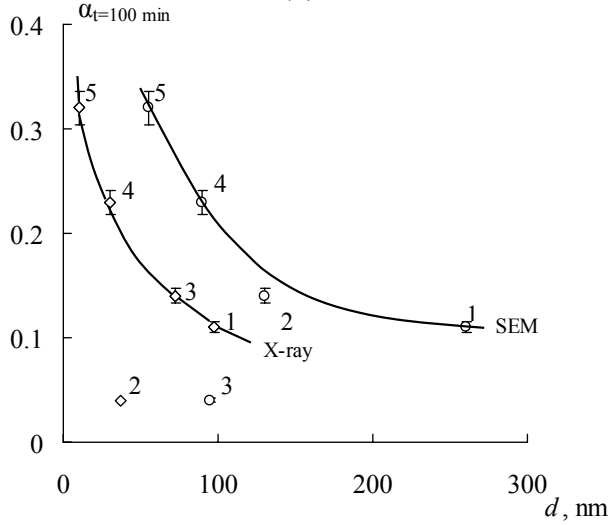

Fig. 5. Dependence of the degree of completeness α of the ROS of molecular oxygen on the mean diameter *d* of a silver particle for process time *t* = 100 min; the dots represent the experimental data for systems *1–5* given in Table 1.

To investigate the rate of oxygen ROS as a function of silver content in NCs, kinetic curves (Fig. 6) were obtained with different capacity of NCs with respect to silver, which was less than ion-exchange capacity. Kinetic curves show direct proportionality of time necessary for the reaction to reach certain degree of completion to the silver content in the pattern (Fig. 7a). With the decrease of silver loading, the rate of oxygen ROS $d\alpha/dt$ is rather increased (Fig. 7b).

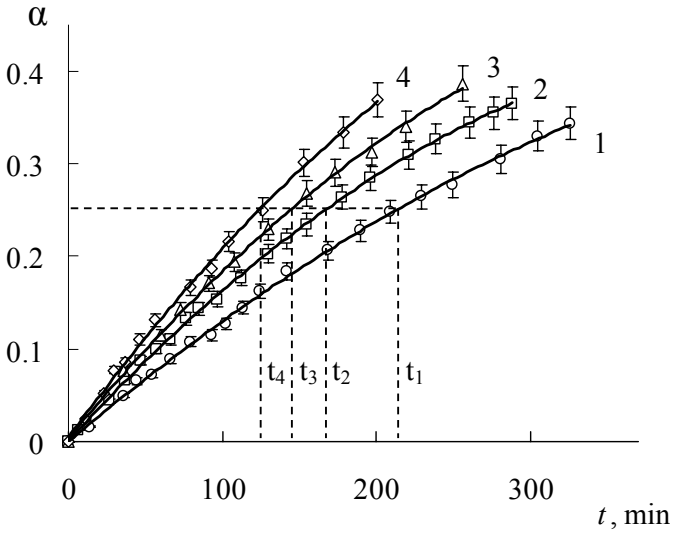

Fig. 6. Kinetic curves for the process completion degree α of the ROS of molecular oxygen from water by Ag^0·KU-23 in H^+-ion form with different capacity with respect to silver ε_{Ag^+}, mmol/cm^3: 1 – 1.02; 2 – 0.76; 3 – 0.62; 4 – 0.58

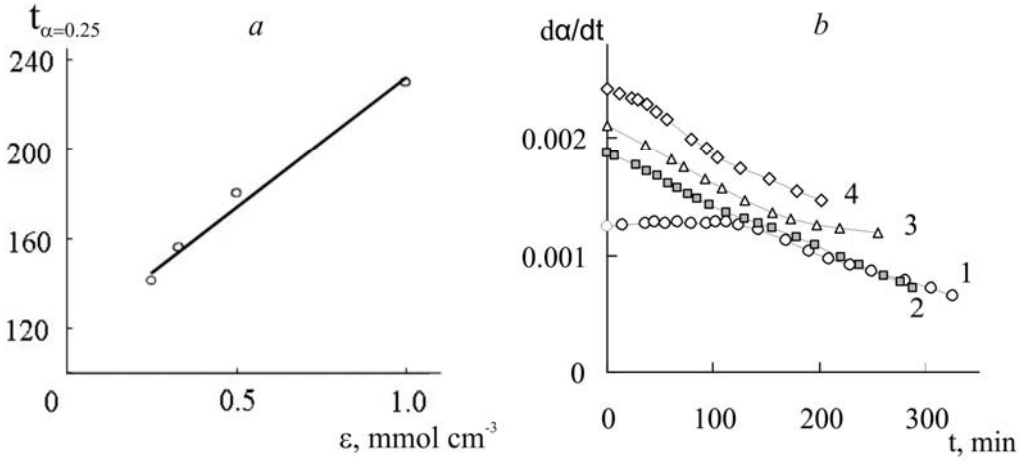

Fig. 7. Time $t_{\alpha=0.25}$ required to reach a 0.25 degree of process completion vs. capacity of Ag^0·KU-23 with respect to silver (*a*) and rate of oxygen ROS $d\alpha/dt$ (*b*) by Ag^0·KU-23 in H^+-ion form with different capacity with respect to silver (curves designations as Fig. 6).

Recently, we have demonstrated [27] that stage of internal oxygen diffusion is not rate-controlling step of ROS process in Ag^0·KU-23. It means that rate rises because of the intensification of the chemical interaction on the silver surface. Probably, silver nanoparticles exhibit the catalytic effect [28], which is strongly marked in the case of silver content less than ion exchange capacity.

Conclusion

Silver-containing NCs that are chemically active towards dissolved oxygen have been obtained. By changing the nature of the precursor and reducing agent, it is possible to control the size of silver particles. The average size of silver particles decreases in a series of precursor compounds AgCl > AgBr > AgI, and reducing agents N_2H_4 > $NaBH_4$ > H_2. The rate of molecular oxygen reduction increases with the decrease of the size of silver

nanoparticles and silver content in the NC. On the one hand, the process is accelerated due to the increased ratio of the surface area to the size of a metal particle. On the other hand, silver exhibits catalytic properties, which are more obvious with low silver content.

This work is supported by the RFBR (Rus. Fund of Basic Research, grant № 11-08-00174_a).

References

1.Nicolais L., Carotenuto G. Metal - Polymer Nanocomposites. N.Y.: Wiley, 2004.304 p.

2.Poole Ch., Owens F. Introduction to Nanotechnology. New Jersey: Wiley, 2003. 400 p.

3.Pomogailo A.D., Rozenberg A.S. Uflyand, I.E. Metal Nanoparticles in Polymers. Khimiya: Moscow, 2000. 672 p.

4.Corain B., M. Zecca, P. Canton, P. Centomo. Synthesis and catalytic activity of metal nanoclusters inside functional resins: an endeavour lasting 15 years // Phil. Trans. R. Soc. A. 2010. V. 368. P. 1495–1507.

5.Zolotukhina E.V., Kravchenko T.A. Synthesis and kinetics of growth of metal nanoparticles inside ion-exchange polymers // Electrochim. Acta. 2011. V. 56. P. 3597–3604.

6.Yaroslavtsev A.B., Nikonenko V.V. Ion-exchange membrane materials: properties, modification, and practical application // Nanotechnol. Russia. 2009. V. 4. P. 137-159.

7.Sergeev G.B. Nanochemistry. Moscow: Mosc. Gos. Univ., 2003. 288 p.

8.Domènech B., Bastos-Arrieta J., Alonso A., Macanás J., Muñoz M., and Muraviev D.N. // Ion Exchange Technologies / Ed. by A. Kilislioğlu. Rijeka: InTech, 2012. P. 35-72.

9.Ruiz P., Muñoz M., Macanás J., Muraviev D.N. Intermatrix synthesis of polymer-stabilized PGM@Cu core–shell nanoparticles with enhanced electrocatalytic properties // React. Funct. Polym. 2011. V. 71. P. 916-924.

10. Kravchenko T.A., Chayka M.Yu., Konev D.V., Polyanskiy L.N., Krysanov V.A. The influence of the ion-exchange groups nature and the degree of chemical activation by silver on the process of copper electrodeposition into the ion exchanger // Electrochim. Acta. 2007. V. 53. P. 330-336.

11. Kravchenko T., Khorolskaya S., Polyanskiy L., Kipriyanova E. Investigation of the mass transfer process in metal-ion-exchanger nanocomposites // Nanocomposites: Synthesis, Characterization and Applications / Ed. by X. Wang. N.Y.: Nova Science Publishers, 2013. P. 329-348.

12. Sarkar S., Chatterjee P.K., Cumball L.H., SenGupta A.K. Hybrid ion exchanger supported nanocomposites: Sorption and sensing for environmental applications // Chem. Eng. J. 2011. V. 166. P. 923–931.

13. Sarkar S., Guibal E., Quignard F., SenGupta A.K. Polymer-supported metals and metal oxide nanoparticles: synthesis, characterization, and applications // J Nanopart. Res. 2012. V. 14: 715.

14. Kuhlmann A., Roessner F., Schwieger W., Gravenhorst O., Selvam T. New bifunctional catalyst based on Pt containing layered silicate Na-ilerit // Catal. Today. 2004. V. 97. P. 303–306.

15. Wang Q., Yu H., Zhong L., Liu J., Sun J., Shen J. Incorporation of silver ions into ultrathin titanium phosphate films: In situ reduction to prepare silver nanoparticles and their antibacterial activity // Chem. Mater. 2006. V. 18. P. 1988-1994.

16. Kravchenko T.A., Polyanskiy L.N., Krysanov V.A., Zelensky E.S., Kalinitchev A.I., Hoell W.H. Chemical precipitation of copper from copper–zinc solutions onto selective sorbents // Hydromet. 2009. V. 95. P. 141–144.

17. Kravchenko T.A., Polyanskiy L.N., Kalinichev A.I., Konev D.V. Metal–Ion Exchanger Nanocomposites. Moscow: Nauka, 2009. 391 p.

18. Kozhevnikov A.V. Electron-Ion Exchangers: A New Group of Redoxites. N.Y.: Wiley, 1975. 129 p.

19. Sinha V., Li K. Alternative methods for dissolved oxygen removal from water: a comparative study // Desalination. 2000. V. 12. P. 155-164.

20. Shi W., Cui C., Zhao L., Yu Sh., Yun X. Removal of dissolved oxygen from water using a Pd-resin based catalytic reactor // Front. Chem. Eng. China. 2009. V. 3. P. 107–111.

21. Grzelczak M., Vermant J., Furst E.M., Liz-Marzan L.M. Directed self-assembly of nanoparticles // ACS Nano. 2010. V. 4. P. 3591–3605.

22. Rostovshchikova T.N., Smirnov V.V., Kozhevin V.M., Yavsin D.A., Gurevich S.A. Intercluster interactions in catalysis by metal nanoparticles // Ross. Nanotekhnol. 2007. V.2 (1-2). P.47-60.

23. Nikolskiy B.P. Chemists Manual. Moscow-Leningrad: Khimiya, 1964. Vol. 3. pp. 229-230.

24. Guo A., Yin X., Fan K., Dai W.L. Influence of copper precursors on the structure evolution and catalytic performance of Cu/HMS catalysts in the hydrogenation of dimethyl oxalate to ethylene glycol // Appl. Catal. 2010. V. 377. P. 128-133.

25. Yang Y., Zhou Y. Particle size effects for oxygen reduction on dispersed silver + carbon electrodes in alkaline solution // J. Electroanal. Chem. 1995. V. 397. P. 271-278.

26. Sviridov V.V. Chemical Deposition of Metals from Aqueous Solutions. Minsk: Universitetskoe, 1987. 270 p.

27. Peshkov S.V., Kravchenko T.A., Konev D.V., Kipriyanova E.S., Chepkova S.P. // Sorbtsion. Khromatogr. Protsessy. 2009. V. 9. I. 2. P. 221-232.

28. Zhang X., Qu Zh.,Yu F.,Wang Y., Zhang X. Effects of pretreatment atmosphere and silver loading on the structure and catalytic activity of Ag/SBA-15 catalysts // J. Mol. Catal. A. 2013. V. 370. P. 160–166.

Khorolskaya Svetlana V. – post-graduated student of Physical Chemistry Department, Voronezh State University, tel. (473) 2208-538, e-mail: khorolskaya@chem.vsu.ru

Peshkov Sergey Vladimirovich – PhD, principal industrial engineer of water treatment department of Hydrogas JSC, Voronezh

Kravchenko Tamara A..– professor of Physical Chemistry Department, Voronezh State University, tel. (473) 2208-538, e-mail: krav@chem.vsu.ru